

# Effects of Rare Earth Nanoparticles ( $M = \text{Sm}_2\text{O}_3, \text{Ho}_2\text{O}_3, \text{Nd}_2\text{O}_3$ ) Addition on the Microstructure and Superconducting Transition of $\text{Bi}_{1.6}\text{Pb}_{0.4}\text{Sr}_2\text{Ca}_2\text{Cu}_3\text{O}_{10+\delta}$ Ceramics (Kesan Penambahan Nanozarah Nadir-Bumi ( $M = \text{Sm}_2\text{O}_3, \text{Ho}_2\text{O}_3, \text{Nd}_2\text{O}_3$ ) ke atas Mikrostruktur dan Peralihan Kesuperkonduksian Seramik $\text{Bi}_{1.6}\text{Pb}_{0.4}\text{Sr}_2\text{Ca}_2\text{Cu}_3\text{O}_{10+\delta}$ )

H. BAGIAH, S.A. HALIM\*, S.K. CHEN, K.P. LIM & M.M. AWANG KECHIK

## ABSTRACT

The effect of rare earth nanoparticles,  $M = \text{Sm}_2\text{O}_3, \text{Nd}_2\text{O}_3$  and  $\text{Ho}_2\text{O}_3$  added to  $(\text{Bi}_{1.6}\text{Pb}_{0.4}\text{Sr}_2\text{Ca}_2\text{Cu}_3\text{O}_{10+\delta})_{1-x}(M)_x$ , where  $x = 0.00 - 0.05$ , superconductor were studied by X-ray diffraction technique (XRD), resistivity ( $R$ ), scanning electron microscopy (SEM) and energy dispersive spectroscopy (EDX). The volume fraction of high- $T_c$  phase, Bi-2223, decreased from 84% for pure sample to 48, 30 and 23% at  $x = 0.05$  for  $\text{Sm}_2\text{O}_3, \text{Ho}_2\text{O}_3$  and  $\text{Nd}_2\text{O}_3$  additions, respectively. The critical temperature  $T_{c(R=0)}$  that is 102 K for the pure sample decreased to 78, 73 and 69 K at  $x = 0.05$  for samples with  $\text{Sm}_2\text{O}_3, \text{Nd}_2\text{O}_3$  and  $\text{Ho}_2\text{O}_3$  nanoparticles additions, respectively. The additions of rare earth nanoparticles decreased the grain size and increased the random orientation of the grains. The results showed that the phases' formations, variations of lattice parameters and electrical properties are sensitive to the size of nanoparticles and magnetic properties of its ions.

**Keywords:** High  $T_c$  phase (Bi-2223); hole concentration; pairing mechanism;  $\text{Sm}_2\text{O}_3, \text{Ho}_2\text{O}_3$  and  $\text{Nd}_2\text{O}_3$  rare earth nanoparticles

## ABSTRAK

Kesan penambahan nanozarah nadir-bumi  $M = \text{Sm}_2\text{O}_3, \text{Nd}_2\text{O}_3$  dan  $\text{Ho}_2\text{O}_3$  ke atas bahan superkonduktor  $(\text{Bi}_{1.6}\text{Pb}_{0.4}\text{Sr}_2\text{Ca}_2\text{Cu}_3\text{O}_{10+\delta})_{1-x}(M)_x$ , dengan  $x = 0.00 - 0.05$ , telah dikaji dengan teknik (XRD), kerintangan ( $R$ ), mikroskopi imbasan elektron (SEM) dan spektroskopi serakan tenaga (EDX). Pecahan isi padu untuk fasa  $T_c$ -tinggi, Bi-2223, berkurangan daripada 84% untuk sampel tulen ke 48, 30 dan 23% pada  $x = 0.05$  untuk penambahan masing-masing  $\text{Sm}_2\text{O}_3, \text{Ho}_2\text{O}_3$  dan  $\text{Nd}_2\text{O}_3$ . Suhu kritikal  $T_{c(R=0)}$  untuk sampel tulen ialah 102 K dan berubah ke 78, 73 dan 69 K pada  $x = 0.05$  untuk sampel yang ditambah dengan nanozarah masing-masing  $\text{Sm}_2\text{O}_3, \text{Nd}_2\text{O}_3$  dan  $\text{Ho}_2\text{O}_3$ . Penambahan nanozarah nadir-bumi mengurangkan saiz butiran dan meningkatkan kerawakan orientasi butiran. Hasil kajian menunjukkan bahawa pembentukan fasa, variasi dalam parameter kekisi dan sifat kekonduksian elektrik adalah peka terhadap saiz nanozarah dan sifat magnet ionnya.

**Kata kunci:** Fasa  $T_c$ -tinggi (Bi-2223); nanozarah nadir-bumi  $\text{Sm}_2\text{O}_3, \text{Ho}_2\text{O}_3$  dan  $\text{Nd}_2\text{O}_3$ ; mekanisme perpasangan; kepekatan lubang

## INTRODUCTION

The BSCCO is a well-known superconductor's material that received great attention from scientific community since they were discovered by (Hiroshi et al. 1988). The superconducting phases in BSCCO system are expressed by a general formula of  $(\text{Bi}, \text{Pb})_2\text{Sr}_2\text{Ca}_{n-1}\text{Cu}_n\text{O}_y$  ( $n = 1, 2, 3$ ), for which the abbreviation Bi2201, Bi2212 and Bi2223 phases are used and their superconducting transition temperatures ( $T_c$ ) are around 20, 85 and 110 K, respectively. The Bi2223 phase is one of the most promising candidates for superconductor technology. The superconducting properties of Bi2223 system are highly related to its hole concentration, pinning ability and its phase structure (Aloysius et al. 2005; Maple 1998; Prabitha et al. 2005; Presland et al. 1991; Terzioglu et al. 2005). The research interest in BSCCO system is mainly concentrated in the enhancement and understanding of overall property

of the Bi2223 phase in order to prepare the material for practical applications.

Chemical doping and addition control the superconducting and physical properties of layered structure superconductors (Aloysius et al. 2005; Maple 1998; Prabitha et al. 2005; Presland et al. 1991; Terzioglu et al. 2005). The doping of Sm ions in Bi2223 system degraded the  $T_c$  and microstructure (Terzioglu et al. 2005). However, the addition of Nd ions enhanced the flux pinning property of the Bi2223 phase (Aloysius et al. 2005).

The addition of nanoparticles in  $\text{Bi}_{1.6}\text{Pb}_{0.4}\text{Sr}_2\text{Ca}_2\text{Cu}_3\text{O}_{10+\delta}$  system is known to enhance its flux pinning ability because their size is comparable to magnetic flux diameter of high temperature superconductors (Abd-Shukor et al. 2008; Wei & Abd-Shukor 2007; Yahya et al. 2004). On the other hand, the addition of nanoparticles is also expected to change other superconducting properties of Bi2223 system

(Abd-Shukor et al. 2008; Garnier et al. 2002; Ghattas et al. 2008; Guilmeau et al. 2003; Guo et al. 1999; Mikhailov et al. 2003; Wei & Abd-Shukor 2007; Yahya et al. 2004). The effects of different rare earth nanoparticles  $\text{Sm}_2\text{O}_3$ ,  $\text{Nd}_2\text{O}_3$  and  $\text{Ho}_2\text{O}_3$  additions on structural and superconducting transition of  $\text{Bi}_{1.6}\text{Pb}_{0.4}\text{Sr}_2\text{Ca}_2\text{Cu}_3\text{O}_{10+\delta}$  system have not yet reported. Hence, the aim of this research was to provide comparative study of the effects of different rare earth oxide,  $\text{M} = \text{Sm}_2\text{O}_3$ ,  $\text{Nd}_2\text{O}_3$  and  $\text{Ho}_2\text{O}_3$  addition on the phase formation, microstructure and critical temperature ( $T_c$ ) of  $\text{Bi}_{1.6}\text{Pb}_{0.4}\text{Sr}_2\text{Ca}_2\text{Cu}_3\text{O}_{10+\delta}$  superconductors.

#### EXPERIMENTAL DETAILS

The samples with chemical composition of  $\text{Bi}_{1.6}\text{Pb}_{0.4}\text{Sr}_2\text{Ca}_2\text{Cu}_3\text{O}_{10+\delta}$  were prepared by solid state reaction technique. High purity powders of  $\text{Bi}_2\text{O}_3$ ,  $\text{PbO}$ ,  $\text{SrCO}_3$ ,  $\text{CaCO}_3$  and  $\text{CuO}$  were weighed using 0.0001 g accuracy balance, followed by mixing and grinding by using mortar and pestle. The powder was calcined and ground twice at  $800^\circ\text{C}$  and  $830^\circ\text{C}$  for 24 h each. The calcined powder was then pressed into pellets of about 13 mm diameter and 2 mm thickness using 5 tones pressure and then sintered at  $850^\circ\text{C}$  for 120 h with one intermediate grinding and pressing at the same force. Thereafter, fine powders of  $(\text{Bi}_{1.6}\text{Pb}_{0.4}\text{Sr}_2\text{Ca}_2\text{Cu}_3\text{O}_{10+\delta})_{1-x}(\text{M})_x$ , with  $x=00, 0.005-0.05$ , were mixed with rare earth nanoparticles,  $\text{M} = \text{Sm}_2\text{O}_3$ ,  $\text{Nd}_2\text{O}_3$  and  $\text{Ho}_2\text{O}_3$  and stirred for the same time including undoped sample in order to ensure identical physical properties. The mixed powders were pressed into cylindrical pellets at applied pressure of 5 tons using hydraulic press. Finally, the pellets were sintered at  $850^\circ\text{C}$  for 30 h in a dedicated tube furnace. The as supplied rare earth nanoparticles of  $\text{Sm}_2\text{O}_3$ ,  $\text{Nd}_2\text{O}_3$  and  $\text{Ho}_2\text{O}_3$  nanoparticles have the size of 14.8, 18 and 49-64 nm, respectively.

The X-ray diffraction measurement (XRD) was carried out by Philips X'Pert Pro diffractometer. Phase analysis of XRD data was done by X'pert high score software. Lattice parameters were calculated by refine the XRD data using nonlinear least square based software. The percentage of Bi2223 phase was calculated using the flowing formula,

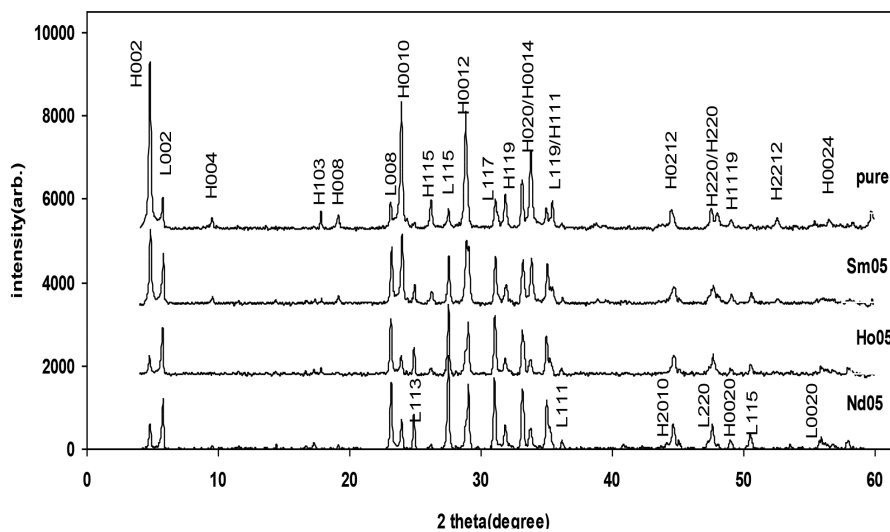
$$V_{\text{Bi2223}}\% = \frac{\sum I_{\text{Bi2223}}}{(\sum I_{\text{Bi2223}} + \sum I_{\text{Bi2212}})} \times 100\%, \quad (1)$$

where  $I_{\text{Bi2223}}$  and  $I_{\text{Bi2212}}$  are the intensity of peaks related to Bi2223, Bi2212, respectively.

Resistivity measurements were done by standard four point probe technique with silver paint contact in order to determine  $T_c$  (onset), where the resistivity start to decrease and  $T_c$  ( $R=0$ ), where the material loose resistivity completely. Scanning electron micrographs were recorded by using a JEOL 6400 SEM with 4500 magnification. The distributions of rare earth nanoparticles in the samples' surface were estimated using Oxford energy dispersive X-ray analyzer coupled with SUPRA55 field emission scanning electron microscopy (FESEM).

#### RESULTS AND DISCUSSION

Figure 1 shows the X-ray diffraction patterns of pure and  $(\text{Bi}_{1.6}\text{Pb}_{0.4}\text{Sr}_2\text{Ca}_2\text{Cu}_3\text{O}_{10})_{0.95}(\text{M})_{0.05}$  samples, where  $\text{M} = \text{Sm}_2\text{O}_3$ ,  $\text{Ho}_2\text{O}_3$  and  $\text{Nd}_2\text{O}_3$  rare earth nanoparticles, respectively. The most intense peaks refer to Bi2223 phase having (00L) direction. The additions of rare earth nanoparticles inhibit the Bi2223 phase formation gradually. It is known that the introduction of Sm and Nd ions in  $\text{Bi}_{1.6}\text{Pb}_{0.4}\text{Sr}_2\text{Ca}_2\text{Cu}_3\text{O}_{10}$  system promoted the formation of Bi2212 phase and decreased the volume of Bi2223 phase (Aloysius et al. 2005; Biju et al. 2007; Terzioglu et al. 2005).



Note: Peaks of the high- $T_c$ , Bi2223, and low- $T_c$ , Bi2212, phases are indexed as H and L, respectively

FIGURE 1. XRD patterns of the  $(\text{Bi}_{1.6}\text{Pb}_{0.4}\text{Sr}_2\text{Ca}_2\text{Cu}_3\text{O}_{10})_{1-x}(\text{M})_x$  samples with  $x=0.05$  where  $\text{M} = \text{Sm}_2\text{O}_3$ ,  $\text{Ho}_2\text{O}_3$  and  $\text{Nd}_2\text{O}_3$  nanoparticles

Figure 2 shows the volume fraction of Bi2223 phase of samples against rare earth nanoparticles addition. The dominant phase, Bi2223, maintains up to  $x = 0.03$  with  $\text{Sm}_2\text{O}_3$  and to  $x = 0.02$  for samples with  $\text{Ho}_2\text{O}_3$  and  $\text{Nd}_2\text{O}_3$ , respectively. The volume fractions of Bi2223 phase at  $x = 0.05$  are 48, 30 and 23% for samples with  $\text{Sm}_2\text{O}_3$ ,  $\text{Ho}_2\text{O}_3$  and  $\text{Nd}_2\text{O}_3$  nanoparticles, respectively. The Bi2223 phase is stable with  $\text{Sm}_2\text{O}_3$  more than those with  $\text{Nd}_2\text{O}_3$  and  $\text{Ho}_2\text{O}_3$ . The solubility of rare earth oxides introduced into Bi2223 system decrease with the increase of its ionic size, which in turn reduce Bi2223 phase formation (Sedky 2009). In our results, the size of nanoparticle plays a role in the formation of Bi2223 phase that decreases as the nanoparticles size increases ( $\text{Sm}_2\text{O}_3$  particle <  $\text{Ho}_2\text{O}_3$  particle <  $\text{Nd}_2\text{O}_3$  particle). Only Bi2212 and Bi2223 phases were detected in our samples by XRD measurements, which suggest that the rare earth nanoparticles may incorporate in BSCCO matrix and slow the conversion of Bi2212 phase to Bi2223 phase during annealing process.

Figure 3(a), 3(b) and 3(c) depicts the effects of rare earth nanoparticles,  $\text{Sm}_2\text{O}_3$ ,  $\text{Ho}_2\text{O}_3$  and  $\text{Nd}_2\text{O}_3$  nanoparticles on the lattice parameters of  $a$  and  $c$  axes. The  $a$  axis increases while  $c$  axis decreases with the additions of rare earth nanoparticles. This behavior may not be explained by the possible substitution of rare earth ion in suitable site like Ca site as reported in Bi2223 doped with rare earth element (Ghattas et al. 2008; Min Soo & Ki Young 2002; Terzioglu et al. 2008). The presence of rare earth oxide nanoparticle about Bi2223 phase unit cell may cause an incorporation of additional Oxygen ion associated with rare earth ions about BiO layer that affect the transferring of holes from charge reservoir (BiO layer) to Cu-O conducting plane (Sarun et al. 2007). This may weakened the Cu-O bond, which causes  $a$ -axis to increase and  $c$ -axis to decrease. EDX analysis indicate that the Oxygen contents increase

in  $(\text{Bi}_{1.6}\text{Pb}_{0.4}\text{Sr}_2\text{Ca}_2\text{Cu}_3\text{O}_{10})_{1-x}(\text{M})_x$  with increase rare earth nanoparticles contents.

Figure 4 shows the surface microstructure of samples added with  $\text{Sm}_2\text{O}_3$ ,  $\text{Nd}_2\text{O}_3$  and  $\text{Ho}_2\text{O}_3$  rare earth nanoparticles. The pure sample has large oriented platelets grains where some of them were oriented toward  $c$ -axis direction. This can also be concluded from XRD data where strong peak with  $(00L)$  orientation were related to the pure sample. The average grain size of pure sample is  $2.7 \mu\text{m}$ . The grains become smaller, more randomly orientated and more porous with the addition of rare earth nanoparticles. Samples with  $x = 0.02$  have 1.3, 1.4 and  $1.1 \mu\text{m}$  average grain size for  $\text{Sm}_2\text{O}_3$ ,  $\text{Nd}_2\text{O}_3$  and  $\text{Ho}_2\text{O}_3$ , respectively.

The distributions of rare earth nanoparticles in samples' surface with  $x=0.05$  were estimated using EDX spectroscopy. Figure 5 shows the distributions of  $\text{Sm}_2\text{O}_3$ ,  $\text{Nd}_2\text{O}_3$  and  $\text{Ho}_2\text{O}_3$  nanoparticles and its mapping in samples' surface. It is obvious that rare earth nanoparticles are homogeneously distributed in BSCCO matrix. Figure 6 shows spectrum regions of EDX measurement in SEM micrograph of the  $(\text{Bi}_{1.6}\text{Pb}_{0.4}\text{Sr}_2\text{Ca}_2\text{Cu}_3\text{O}_{10})_{1-x}(\text{M})_x$  samples with  $x=0.05$  where  $\text{M} = \text{Sm}_2\text{O}_3$ ,  $\text{Ho}_2\text{O}_3$  and  $\text{Nd}_2\text{O}_3$  nanoparticles. Table 1 listed the average atomic concentrations percentage of composite element of samples from 1, 2 and 3 spectrum regions. The estimated chemical formula of samples has been calculated by assume the stoichiometric ratio of Bi atoms is nearly 1.6 i.e. same as in starting material formula. The estimated formula for samples added with  $\text{Sm}_2\text{O}_3$ ,  $\text{Ho}_2\text{O}_3$  and  $\text{Nd}_2\text{O}_3$  are  $\text{Bi}_{1.6}\text{Pb}_{0.26}\text{Sr}_{1.78}\text{Ca}_{1.7}\text{Cu}_{3.01}\text{O}_{12.23} - (\text{Sm}_{0.047})$ ,  $\text{Bi}_{1.6}\text{Pb}_{0.25}\text{Sr}_{1.84}\text{Ca}_{1.53}\text{Cu}_{2.92}\text{O}_{13.65} - (\text{Ho}_{0.09})$  and  $\text{Bi}_{1.6}\text{Pb}_{0.41}\text{Sr}_{1.91}\text{Ca}_{1.99}\text{Cu}_{3.04}\text{O}_{14.42} - (\text{Nd}_{0.1})$ . By comparing the estimated chemical formula of the samples with that of starting materials formula i.e.  $(\text{Bi}_{1.6}\text{Pb}_{0.4}\text{Sr}_2\text{Ca}_2\text{Cu}_3\text{O}_{10})_{0.95}(\text{M})_{0.05}$ , where  $\text{M} = \text{Sm}_2\text{O}_3$ ,  $\text{Ho}_2\text{O}_3$  and  $\text{Nd}_2\text{O}_3$ , it can be concluded that the samples has an excess of oxygen content.

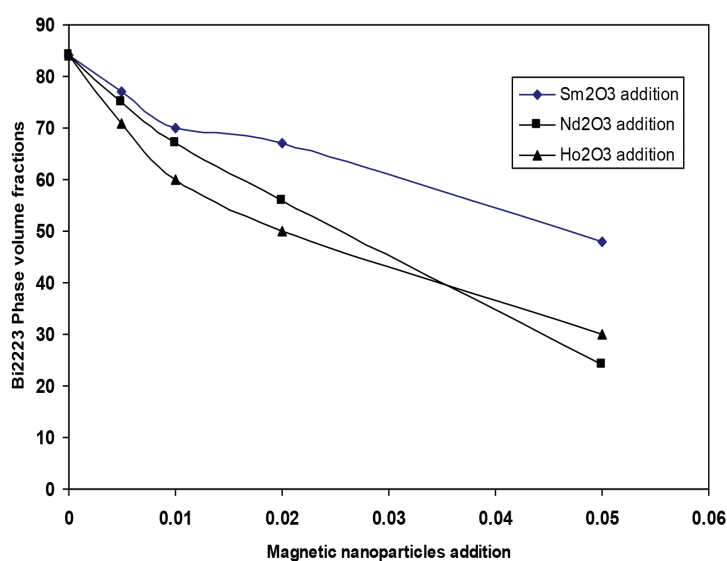


FIGURE 2. The volume fraction of Bi2223 phase against magnetic nanoparticles addition

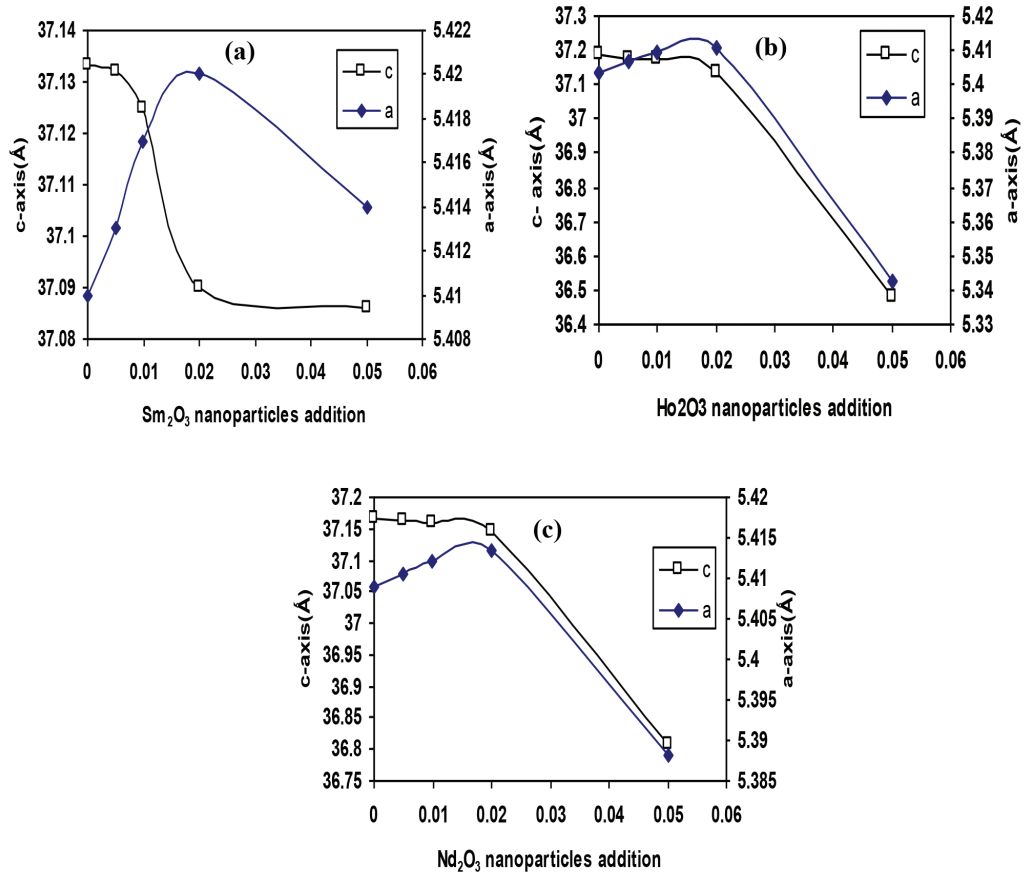


FIGURE 3. Lattice parameter *a* and *b* axes of Bi2223 phase against (a) Sm<sub>2</sub>O<sub>3</sub>, (b) Ho<sub>2</sub>O<sub>3</sub> and (c) Nd<sub>2</sub>O<sub>3</sub> nanoparticles addition

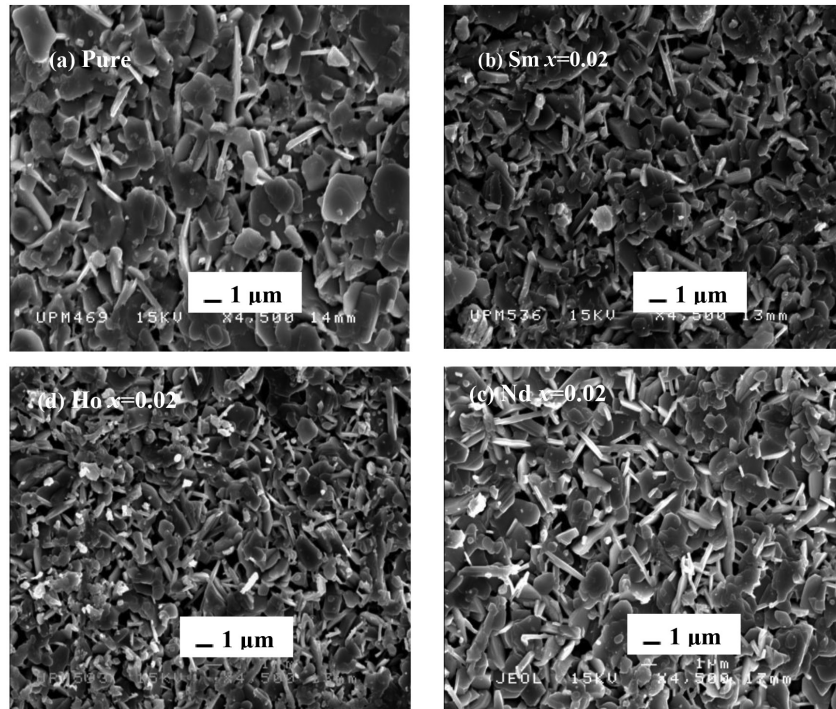


FIGURE 4. SEM micrograph for pure (Bi<sub>1.6</sub>Pb<sub>0.4</sub>Sr<sub>2</sub>Ca<sub>2</sub>Cu<sub>3</sub>O<sub>10</sub>) and after added with (b) Sm<sub>2</sub>O<sub>3</sub>, (c) Ho<sub>2</sub>O<sub>3</sub> and (d) Nd<sub>2</sub>O<sub>3</sub> rare earth nanoparticles

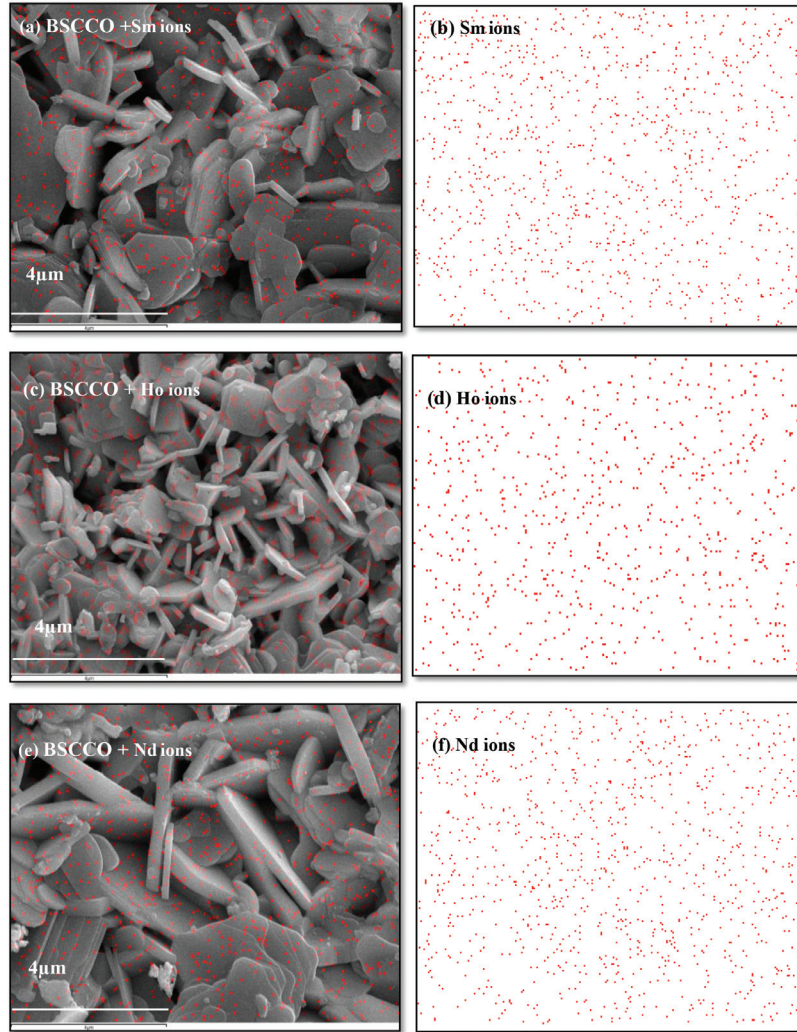


FIGURE 5. The mapping and distribution of (a) Sm, (c) Nd and (e) Ho ions in BSCCO matrix and mapping of (b) Sm, (d) Nd and (f) Ho ions with different contrast color

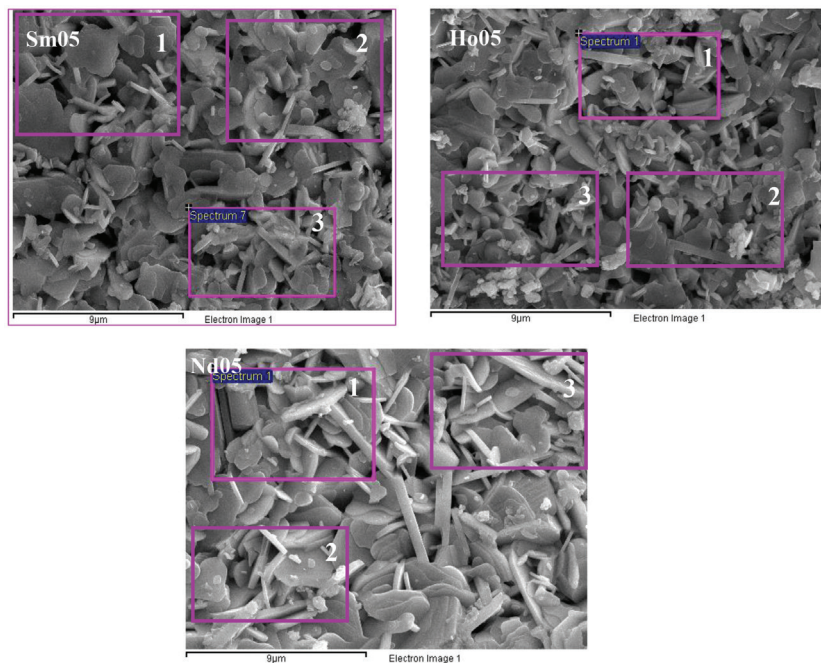


FIGURE 6. Spectrum region of EDX measurement in SEM micrograph of the  $(\text{Bi}_{1.6}\text{Pb}_{0.4}\text{Sr}_2\text{Ca}_2\text{Cu}_3\text{O}_{10})_{1-x}(\text{M})_x$  samples with  $x = 0.05$  where  $\text{M} = \text{Sm}_2\text{O}_3$ ,  $\text{Ho}_2\text{O}_3$  and  $\text{Nd}_2\text{O}_3$  nanoparticles

TABLE 1. Average of atomic concentration from spectrum of 1, 2 and 3 region of the  $(\text{Bi}_{1.6}\text{Pb}_{0.4}\text{Sr}_2\text{Ca}_2\text{Cu}_3\text{O}_{10})_{1-x}(\text{M})_x$  samples with  $x=0.05$  where  $\text{M}=\text{Sm}_2\text{O}_3$ ,  $\text{Ho}_2\text{O}_3$  and  $\text{Nd}_2\text{O}_3$  nanoparticles

Element	Average Atomic concentration% with $(\text{Sm}_2\text{O}_3$ addition) from 1, 2, and 3 spectrum %	Average Atomic concentration% with $(\text{Ho}_2\text{O}_3$ addition) from 1, 2, and 3 spectrum %	Average Atomic concentration % with $(\text{Nd}_2\text{O}_3$ addition) from 1, 2, and 3 spectrum %
O K	59.30	62.36	61.45
Ca K	8.24	6.97	8.48
Cu K	14.60	13.35	12.94
Sr L	8.65	8.43	8.14
Sm L	0.23	-	-
Ho L	-	0.427	-
Nd L	-	-	0.44
Pb M	1.24	1.15	1.76
Bi M	7.75	7.33	6.80

Figure 7 shows the resistance versus temperature measurements carried out from 55 K to 270 K for pure and  $(\text{Bi}_{1.6}\text{Pb}_{0.4}\text{Sr}_2\text{Ca}_2\text{Cu}_3\text{O}_{10})_{0.95}(\text{M})_{0.05}$  samples where  $\text{M}=\text{Sm}_2\text{O}_3$ ,  $\text{Ho}_2\text{O}_3$  and  $\text{Nd}_2\text{O}_3$  rare earth nanoparticles. The critical temperature,  $T_c$ , decreased with introduction of rare earth nanoparticles in  $\text{Bi}_{1.6}\text{Pb}_{0.4}\text{Sr}_2\text{Ca}_2\text{Cu}_3\text{O}_{10}$  system. The pure sample has single step transition indicating that the sample is dominated by Bi2223 phase. On the other hand, the samples with  $x = 0.05$  have double stage transition implying that the sample have two superconducting phases as confirmed from XRD result.

Figure 8 and Figure 9 show more details of critical temperature suppression via rare earth nanoparticles addition. The critical temperature,  $T_c$  onset, does not change in the range  $x = 0.00 - 0.01$ , with  $\text{Sm}_2\text{O}_3$  addition and in the range  $0.005 - 0.1$  with  $\text{Ho}_2\text{O}_3$  and  $\text{Nd}_2\text{O}_3$  addition, which may be due the fact that the samples have dominant

by Bi2223 phase (Figure 8). In the range  $x = 0.02 - 0.05$ , the  $T_c$  onset becomes lower which may associated with reduction and structural modification of Bi2223 phase which already concluded from XRD analysis.

Figure 9 shows the critical temperature  $T_c$  ( $R=0$ ) against rare earth nanoparticles addition. The value of  $T_c$  ( $R=0$ ) of  $\text{Bi}_{1.6}\text{Pb}_{0.4}\text{Sr}_2\text{Ca}_2\text{Cu}_3\text{O}_{10}$  are known to be affected by the growth of Bi2223 and Bi2212 phases and possibly by the changes of Bi2223 phase lattice parameters caused by the addition of different type of rare earth nanoparticles (Min Soo & Ki Young 2002; Sedky 2009; Terzioglu et al. 2008, 2005; Wei & Abd-Shukur 2007). It can be noticed that the  $T_c$  ( $R=0$ ) reduces in the range  $0.00 - 0.02$  more than those in the range  $0.02 - 0.05$ .

The critical temperature of doped superconductors has relation with hole concentration in the samples. The hole concentrations of doped superconductors can be calculated

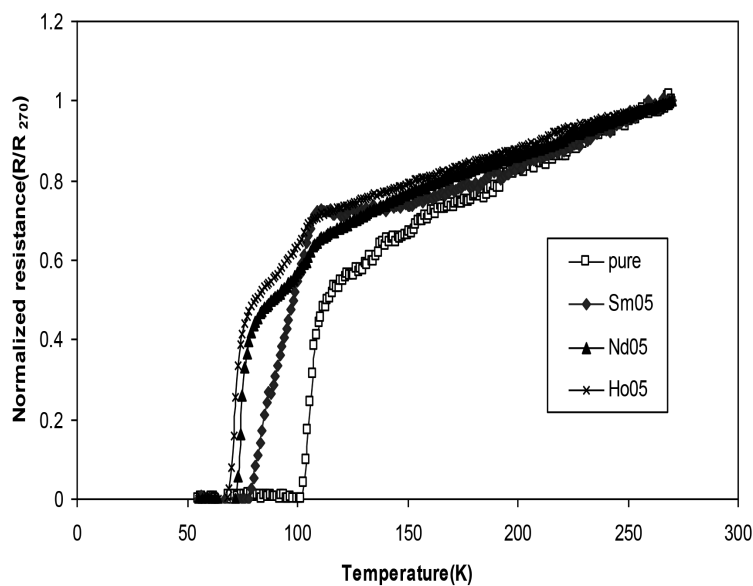


FIGURE 7. Resistance vs. temperature of  $(\text{Bi}_{1.6}\text{Pb}_{0.4}\text{Sr}_2\text{Ca}_2\text{Cu}_3\text{O}_{10})_{0.95}(\text{M})_{0.05}$  where  $\text{M}=\text{Sm}_2\text{O}_3$ ,  $\text{Nd}_2\text{O}_3$  and  $\text{Ho}_2\text{O}_3$  magnetic nanoparticles, respectively

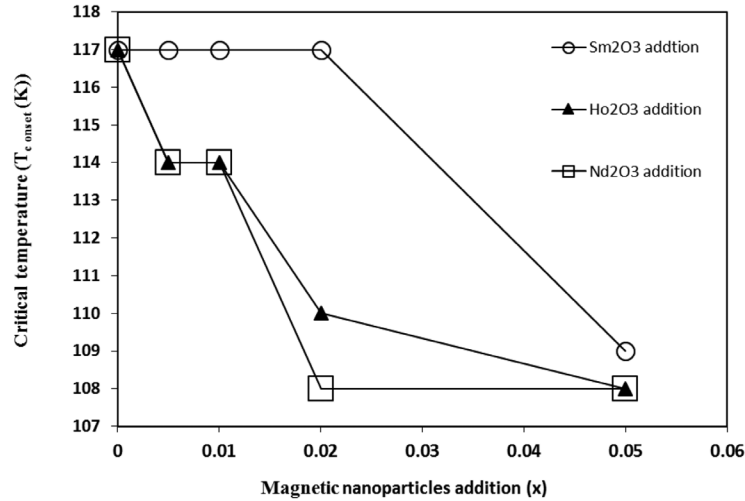


FIGURE 8. The critical temperature  $T_{c\ onset}$  of  $(\text{Bi}_{1.6}\text{Pb}_{0.4}\text{Sr}_2\text{Ca}_2\text{Cu}_3\text{O}_{10-x})(\text{M})_x$  with  $x = 0.0-0.05$ , where  $\text{M} = \text{Sm}_2\text{O}_3, \text{Nd}_2\text{O}_3$  and  $\text{Ho}_2\text{O}_3$  nanoparticles

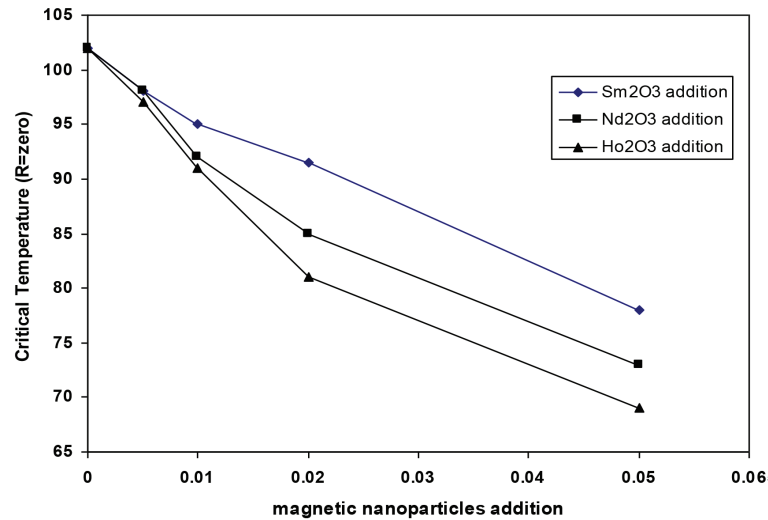


FIGURE 9. The critical temperature  $T_c (R=0)$  of  $(\text{Bi}_{1.6}\text{Pb}_{0.4}\text{Sr}_2\text{Ca}_2\text{Cu}_3\text{O}_{10-x})(\text{M})_x$  with  $x = 0.0-0.05$ , where  $\text{M} = \text{Sm}_2\text{O}_3, \text{Nd}_2\text{O}_3$  and  $\text{Ho}_2\text{O}_3$  nanoparticles

using equation 2 (Presland et al. 1991; Terzioglu et al. 2005).

$$P = 0.16 - \left[ \left( 1 - \frac{T_c}{T_c^{\max}} \right) / 82.6 \right]^{1/2}, \quad (2)$$

where  $T_c$  is the critical temperature of the materials and the  $T_c^{\max}$  is the maximum critical temperature of the materials, which is 110 K for Bi2223 system. Table 2 listed the calculated hole concentrations per  $\text{CuO}_2$  planes.

The increase of  $a$ -axis in samples with  $0.0 < x \leq 0.02$  may result from the  $\text{Cu-O}$  bond weakened due to the reduction in hole concentration in rare earth added  $\text{Bi}_{1.6}\text{Pb}_{0.4}\text{Sr}_2\text{Ca}_2\text{Cu}_3\text{O}_{10}$  system as indicated from XRD

results. The distortion of Bi2223 lattice parameters due to hole concentration reduction was also suggested by (Min Soo & Ki Young 2002; Terzioglu et al. 2008; Sedky 2009).

## CONCLUSION

The effects of rare earth nanoparticles on the microstructure and superconducting transition of  $\text{Bi}_{1.6}\text{Pb}_{0.4}\text{Sr}_2\text{Ca}_2\text{Cu}_3\text{O}_{10}$  ceramic with  $x = 0.0 - 0.02$  and  $0.05$  were investigated. The Bi2223 phase is dominant up to  $x = 0.03$  for  $\text{Sm}_2\text{O}_3$  and to  $x = 0.02$  for  $\text{Nd}_2\text{O}_3$  and  $\text{Ho}_2\text{O}_3$  rare earth nanoparticle, respectively. The  $a$ -axis of Bi2223 phase increases and  $c$ -axis decrease for  $0.0 - 0.02$  and further, decreased strongly with  $x = 0.05$ . The addition of rare earth nanoparticle increases the amount of random orientation platelet grains and decreases its grain size. The rare earth nanoparticles

TABLE 2. Hole concentrations of  $(\text{Bi}_{1.6}\text{Pb}_{0.4}\text{Sr}_2\text{Ca}_2\text{Cu}_3\text{O}_{10})_{1-x}(\text{M})_x$  samples with  $x = 0.0-0.05$ , where  $\text{M} = \text{Sm}_2\text{O}_3$ ,  $\text{Ho}_2\text{O}_3$  and  $\text{Nd}_2\text{O}_3$  nanoparticle

Holes/ $\text{CuO}_2$ planes for samples with	Rare earth nanoparticles	$\text{Sm}_2\text{O}_3$ addition	$\text{Ho}_2\text{O}_3$ addition	$\text{Nd}_2\text{O}_3$ addition
$x = 00$			0.13	
$x = 0.005$		0.124	0.122	0.124
$x = 0.01$		0.118	0.114	0.115
$x = 0.02$		0.116	0.104	0.108
$x = 0.05$		0.101	0.093	0.096

have been homogeneously distributed in BSCCO matrix. The estimated formula for  $\text{Bi}_{1.6}\text{Pb}_{0.4}\text{Sr}_2\text{Ca}_2\text{Cu}_3\text{O}_{10}$  added with  $\text{Sm}_2\text{O}_3$ ,  $\text{Ho}_2\text{O}_3$  and  $\text{Nd}_2\text{O}_3$  are  $\text{Bi}_{1.6}\text{Pb}_{0.26}\text{Sr}_{1.78}\text{Ca}_{1.7}\text{Cu}_{3.01}\text{O}_{12.23} - (\text{Sm}_{0.047})$ ,  $\text{Bi}_{1.6}\text{Pb}_{0.25}\text{Sr}_{1.84}\text{Ca}_{1.53}\text{Cu}_{2.92}\text{O}_{13.65} - (\text{Ho}_{0.09})$  and  $\text{Bi}_{1.6}\text{Pb}_{0.41}\text{Sr}_{1.91}\text{Ca}_{1.99}\text{Cu}_{3.04}\text{O}_{14.42} - (\text{Nd}_{0.1})$ . The maximum decreasing in critical temperature  $T_c$  was found with  $\text{Ho}_2\text{O}_3$  nanoparticle addition, which could be resulted from the strongest magnetic properties of Ho ions. The Bi2223 phase are more stable and superconducting transition,  $T_c$ , of  $\text{Bi}_{1.6}\text{Pb}_{0.4}\text{Sr}_2\text{Ca}_2\text{Cu}_3\text{O}_{10}$  system have the least reduction in the case of  $\text{Sm}_2\text{O}_3$  nanoparticles additions.

#### ACKNOWLEDGMENTS

This research has been supported by the Ministry of Science, Technology and Innovation (MOSTI), Malaysia under grant number 5523132 and the saga grant 5486510.

#### REFERENCES

- Abd Shukor, R., Kechik, M.M.A. & Halim, S.A. 2008. Transport critical current density of Bi-Sr-Ca-Cu-O/Ag superconductor tapes with addition of  $\text{Fe}_3\text{O}_4$  as flux pinning center. *Journal of Physics: Conference Series* 97(1): 012050.
- Aloysius, R.P., Guruswamy, P. & Syamaprasad, U. 2005. Highly enhanced critical current density in Pr-added (Bi, Pb)-2212 superconductor. *Superconductor Science and Technology* 18(5): L23.
- Biju, A., Sarun, P.M., Aloysius, R.P. & Syamaprasad, U. 2007. Structural and superconducting properties of neodymium added  $(\text{Bi,Pb})_2\text{Sr}_2\text{CaCu}_2\text{O}_y$ . *Materials Research Bulletin* 42(12): 2057-2066.
- Garnier, V., Marinel, S. & Desgardin, G. 2002. Influence of the addition of  $\text{SnO}_2$  nano-particles on Bi-2223 phase formation. *Journal of Materials Science* 37(9): 1785-1788.
- Ghattas, A., Annabi, M., Zouaoui, M., Ben Azzouz, F. & Ben Salem, M. 2008. Flux pinning by Al-based nano particles embedded in polycrystalline (Bi,Pb)-2223 superconductors. *Physica C: Superconductivity* 468(1): 31-38.
- Guilmeau, E., Andrzejewski, B. & Noudem, J.G. 2003. The effect of  $\text{MgO}$  addition on the formation and the superconducting properties of the Bi2223 phase. *Physica C: Superconductivity* 387(3-4): 382-390.
- Guo, Y.C., Tanaka, Y., Kuroda, T., Dou, S.X. & Yang, Z.Q. 1999. Addition of nanometer SiC in the silver-sheathed Bi2223 superconducting tapes. *Physica C: Superconductivity* 311(1-2): 65-74.
- Hiroshi, M., Yoshiaki, T., Masao, F. & Toshihisa, A. 1988. A new high- $T_c$  oxide superconductor without a rare earth element. *Japanese Journal of Applied Physics* 27(2A): L209.
- Kittel, C. 1996. *Introduction to Solid State Physics*. New York: John Wiley & Sons. pp. 424-425.
- Maple, M.B. 1998. High-temperature superconductivity. *Journal of Magnetism and Magnetic Materials* 177-181(Part 1): 18-30.
- Mikhailov, B.P., Ichkitidze, L.P., Grigorashvili, Y.E., Mikhailova, A.B. & Shamrai, V.F. 2003. Preparation, structure, and properties of  $(\text{Bi,Pb})_2\text{Sr}_2\text{Ca}_2\text{Cu}_3\text{O}_{10+\delta}$  ceramics with Si3N4 additions. *Inorganic Materials* 39(7): 749-754.
- Min Soo, L. & Ki Young, S. 2002. Effect of Nd substitution for the Ca site in the 110 K phase of (Bi,Pb)-Sr-Ca-Cu-O superconductors. *Superconductor Science and Technology* 15(6): 851.
- Prabitha, V.G., Biju, A., Abhilash Kumar, R.G., Sarun, P.M., Aloysius, R.P. & Syamaprasad, U. 2005. Effect of Sm addition on (Bi, Pb)-2212 superconductor. *Physica C: Superconductivity* 433(1-2): 28-36.
- Presland, M.R., Tallon, J.L., Buckley, R.G., Liu, R.S. & Flower, N.E. 1991. General trends in oxygen stoichiometry effects on  $T_c$  in Bi and Tl superconductors. *Physica C: Superconductivity* 176(1-3): 95-105.
- Sarun, P.M., Biju, A., Guruswamy, P. & Syamaprasad, U. 2007. Enhanced flux pinning of an Nd-added (Bi,Pb)-2212 superconductor. *Journal of the American Ceramic Society* 90(10): 3138-3141.
- Sedky, A. 2009. The impact of Y substitution on the 110 K high  $T_c$  phase in a Bi (Pb):2223 superconductor. *Journal of Physics and Chemistry of Solids* 70(2): 483-488.
- Terzioglu, C., Aydin, H., Ozturk, O., Bekiroglu, E. & Belenli, I. 2008. The influence of Gd addition on microstructure and transport properties of Bi-2223. *Physica B: Condensed Matter* 403(19-20): 3354-3359.
- Terzioglu, C., Yilmazlar, M., Ozturk, O. & Yanmaz, E. 2005. Structural and physical properties of Sm-doped  $\text{Bi}_{1.6}\text{Pb}_{0.4}\text{Sr}_2\text{Ca}_{2-x}\text{Sm}_x\text{Cu}_3\text{O}_y$  superconductors. *Physica C: Superconductivity* 423(3-4): 119-126.
- Wei, K. & Abd-Shukor, R. 2007. Superconducting and transport properties of (Bi-Pb)-Sr-Ca-Cu-O with nano- $\text{Cr}_2\text{O}_3$  additions. *Journal of Electronic Materials* 36(12): 1648-1651.
- Yahya, S.Y., Jumali, M.H., Lee, C.H. & Abd Shukor, R. 2004. Effects of  $\gamma\text{-Fe}_2\text{O}_3$  on the transport critical current density of  $\text{Bi}_{1.6}\text{Pb}_{0.4}\text{Sr}_2\text{Ca}_2\text{Cu}_3\text{O}_{10}$  superconductors. *Journal of Materials Science* 39(23): 7125-7128.

Superconductors and Thin Film Laboratory  
Department of Physics, Faculty of Science  
43400 Serdang, Selangor Darul Ehsan  
Malaysia

\*Corresponding author; email: ahalim@upm.edu.my

Received: 25 March 2015

Accepted: 12 October 2015